High-Z L-Subshell X-Ray Emission Rates*

P. Venugopala Rao, J. M. Palms, and R. E. Wood
Emory University, Atlanta, Georgia 30322
(Received 8 September 1970)

Relative intensities of L x rays emitted during the radiative decay of L_2 and L_3 subshell vacancies are investigated by Si(Li) x-ray detectors, over a range of $65 \leq Z \leq 94$. Intensities of transitions involving N, O, ... electrons compared to those involving M-shell electrons are found to be slightly underestimated in Scofield's theoretical calculations. L_1 subshell yields for $Z = 82$ are measured by a high-resolution study of the Pb L-x-ray spectrum from the decay of ^{207}Bi with the following results: $\omega_1 = 0.09 \pm 0.02$, $f_{12} = 0.17 \pm 0.05$, $f_{13} = 0.61 \pm 0.08$, and $s_1 = 0.353 \pm 0.053$.

I. INTRODUCTION

Interest has developed recently in the measurement of relative intensities of x rays resulting from the filling of inner-shell atomic vacancies. The major impetus for this interest is the availability of high-resolution and high-efficiency semiconductor x-ray detectors. In addition, refined theoretical calculations of the radiative decay rates of atomic-shell vacancies are available from the works of Scofield[1] and Rosner and Bhalla.[2] The experimental results available, however, have been confined to the K-shell vacancy decay rates,[3-7] apparently because of the basic simplicity of the K-series x-ray spectrum. In the present work, the experimental study is extended to the L subshells. Using both singles and coincidence techniques, relative intensities of L x rays from L_2 and L_3 subshells in high-Z elements are measured. Information has also been obtained on the L_1 subshell for $Z = 82$.

The difficulty with the study of L-x-ray spectra is the simultaneous presence of x rays characteristic of all three L subshells. The separation between the subshell edges is very small even at high Z (e.g., 4.6 keV between L_1 and L_3 subshell edges at $Z = 92$). Furthermore the binding energies of the outer-shell electrons that jump in to fill the L-shell vacancies are also of the order of a few keV or less. Consequently, several L x rays of closely spaced energies fall under one photopeak even with the best resolution semiconductor detectors available. Within the present limits of resolution, L-x-ray spectra can be resolved into three main groups, $L\alpha$, $L\beta$, and $L\gamma$ in most of the middle- and high-Z region. The weak lines Ll and $L\eta$ will also be resolved at higher Z, while the $L\beta$ and $L\gamma$ groups will exhibit structure and even resolve into separate components in the transuranium region. Typical L-x-ray spectra taken at two Z values bordering the region of the present study are presented in Fig. 1.

A summary of the most prominent L x rays from each of the three L subshells is given by Bearden.[8] In order to facilitate the analysis of the present work, we define the radiative decay branching ratios s_i for each subshell L_i. For the L_1 subshell, we define

$$s_1 = \frac{I(L_1 - N) + I(L_1 - O) + \cdots}{I(L_1 - M)} = \frac{\text{Intensity of } L\gamma \text{ x rays originating from } L_1 \text{ vacancies}}{\text{Intensity of } L\beta \text{ x rays originating from } L_1 \text{ vacancies}}, \tag{1}$$

where $I(L_1 - X)$ is the intensity of radiative transitions by X-shell electrons filling the L_1 vacancies. Similarly, we have

$$s_2 = \frac{I(L_2 - N) + I(L_2 - O) + \cdots}{I(L_2 - M)} = \frac{\text{Intensity of } L\gamma \text{ x rays originating from } L_2 \text{ vacancies}}{\text{Intensity of } L\eta \text{ and } L\beta \text{ x rays originating from } L_2 \text{ vacancies}}, \tag{2}$$

$$s_3 = \frac{I(L_3 - N) + I(L_3 - O) + \cdots}{I(L_3 - M)} = \frac{\text{Intensity of } L\beta \text{ x rays originating from } L_3 \text{ vacancies}}{\text{Intensity of } Ll \text{ and } L\alpha \text{ x rays originating from } L_3 \text{ vacancies}}. \tag{3}$$

It should be emphasized that the definition of these branching ratios takes into account the fact that the semiconductor x-ray detectors currently available have limited resolution. Obviously, the studies of L-x-ray spectra based on work with bent-crystal-diffraction spectrometers capable of finer resolution need not be confined to the use of such gross ratios of groups of x rays.

The present work is confined to the use of radioactive isotopes, in which electron capture and in-

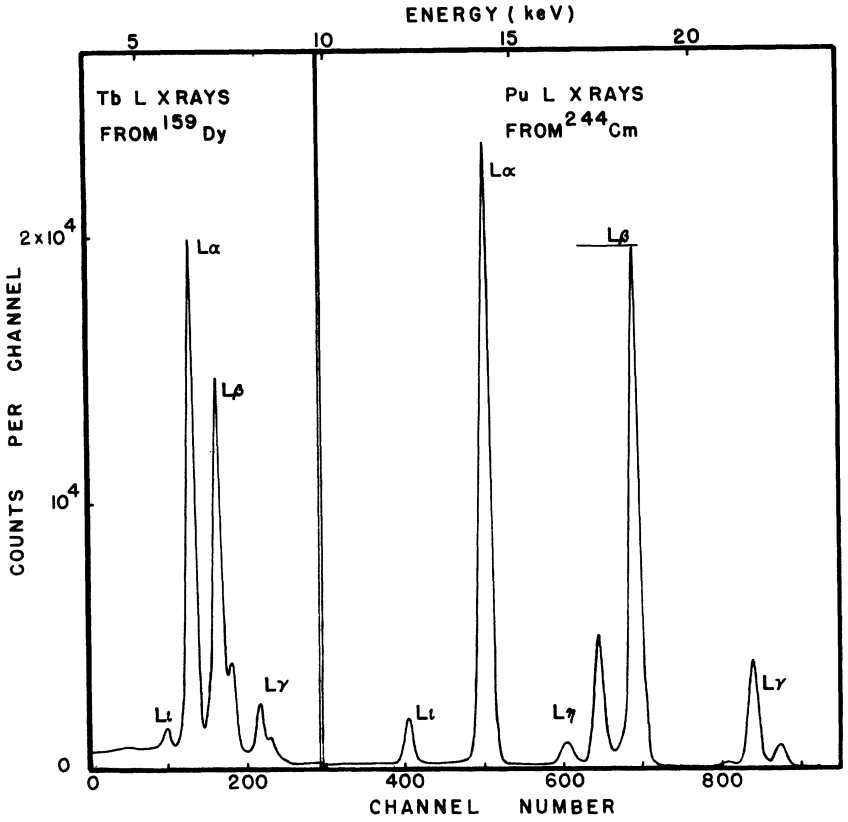

FIG. 1. Singles L-x-ray spectra from the decay of ^{159}Dy and ^{244}Cm taken with a KeVex Si(Li) x-ray spectrometer having a resolution of 220 eV FWHM at 6.4 keV.

ternal conversion produce L vacancies in all the subshells. However, an examination of Fig. 2 reveals the fact that the two lowest-energy photopeaks (Ll and $L\alpha$) are entirely characteristic of the L_3 subshell; thus a singles spectrum analysis is all that is necessary to obtain the relative intensities of Ll and $L\alpha$ x rays arising from the L_3 subshell.

In order to study the x-ray emission from each subshell separately, we need to use coincidence techniques to isolate events leading to the formation of vacancies in one subshell only. The general principles for the application of coincidence techniques to study the individual L subshells were described earlier by one of the authors.[9] These techniques have already been used advantageously to measure both the fluorescence and Coster-Kronig yields of L shells using radioactive sources of L vacancies.[10–16] The procedure is to signal the formation of L_2- or L_3-subshell vacancies by detecting $K\alpha_2$ or $K\alpha_1$ x rays that are emitted during K-L_2 and K-L_3 x-ray transitions, respectively. Thus, L-x-ray spectra observed in coincidence with $K\alpha_1$ x rays are characteristic of the L_3 subshell and those observed in coincidence with $K\alpha_2$ x rays are characteristic of the L_2 subshell. In the latter case, the L_2-L_3X Coster-Kronig transitions have to be taken into account as demonstrated first by Rao and Crasemann.[17] Unfortunately, there is no way of signaling the formation of individual L_1 vacancies by K x rays because the K-L_1 transition is forbidden. But the high-energy end of the L-x-ray spectra should be purely characteristic of the L_1 subshell and it should be possible to study the shape and intensity of $L\gamma$-x-ray peaks arising from the L_1 subshell if sufficient resolution is available. A state of the art resolution study of the Pb L-x-ray spectrum from ^{207}Bi decay is made and the branching ratio s_1, the fluorescence yield ω_1, and Coster-Kronig yields f_{1j}, for the L_1 subshell at $Z = 82$, are determined.

II. EXPERIMENTAL

Radioactive isotopes, carrier free when available, were used as sources of atomic-shell vacancies. Thin sources were made by evaporating a drop of radioactive solution on Mylar film with the following isotopes: ^{159}Dy, ^{171}Tm, ^{181}W, ^{191}Os, ^{186}Re, ^{207}Bi, and ^{210}Pb. Sources of transuranium isotopes ^{238}Pu, ^{241}Am, and ^{244}Cm were prepared by electroplating on thin stainless-steel disks.

The singles L-x-ray spectra were taken with three different Si(Li) detectors of different resolution. All these have almost flat response for photopeak detection in the energy range of interest, i.e., 6–22 keV, thus ideally suited for measurement of relative L-x-ray intensities. A KeVex Si(Li) spectrometer, having a resolution of 260 eV full width

at half-maximum (FWHM) at 6.4 keV (depletion depth 4 mm and active area 30 mm^2) and enclosed in a housing having a 2-mil Be window, was used to study most of the singles spectra. The photopeak detection efficiency of this detector was carefully measured using calibrated sources using the method described elsewhere.[18] A second KeVex Si(Li) x-ray detector with a resolution of 220 eV FWHM at 6.4 keV was employed when better resolution was desired to separate Ll and $L\alpha$ photopeaks. Typical L-x-ray spectra taken with this 220-eV FWHM detector are presented in Fig. 1. The photopeak of the Ll x rays stands clearly on a flat continuum in the high-Z spectrum but at low Z it rests on the slightly sloping low-energy tail of the $L\alpha$ photopeak. The shape of this tail is experimentally determined and subtracted to obtain the true photopeak intensity of Ll x rays.

The Pb L-x-ray spectrum from the electron capture decay of ^{207}Bi (Fig. 2) was taken with a KeVex Si(Li) detector of 10 mm^2 active area and 3 mm thickness having a 2-mil Be window. The spectrum was taken at a counting rate of 200 counts/sec using a KeVex 2002 preamplifier and a KeVex 4000-P amplifier incorporating a pulse optical feedback feature.[19] The detector system has a resolution of 155 eV FWHM for Mn $K\alpha$ x rays (5.9 keV) from the decay of ^{55}Fe.

L-x-ray–K-x-ray coincidences were measured using a fast coincidence system having a resolving time of $2\tau = 80$ nsec. The L x rays were observed with the 260-eV FWHM detector described above while the K x rays were detected with a Ge(Li) detector having a resolution of 470 eV FWHM at 6.4 keV.[20] The analysis of coincidence spectra was carried out according to the procedure outlined in Refs. 10 and 11. Care was taken to correct for the effect of the L_2-L_3 Coster-Kronig transitions in determining the branching ratio s_2 for the radiative decay of L_2-subshell vacancies in the L-x-ray–$K\alpha_2$-x-ray coincidence measurements. In the present work, L_2 and L_3 vacancies at $Z = 76$ and 77 were investigated from the decays of ^{186}Re and ^{191}Os, respectively.

The relative intensities of L x rays in singles as well as coincidence spectra were obtained by correcting the counting rates in the appropriate photopeaks for the photopeak detection efficiency of the detectors, attenuation in air, and other absorbers present. In cases where large accompanying β radiation is present, a thin lucite plate had to be used to stop the β's from flooding the detector. An additional quantity I_L, the total number of L x rays emitted per decay of ^{207}Bi, was also determined by measuring the ratio of intensities of L x rays to K x rays with the Si(Li) detector and the ratio of intensities of K x rays to 570-keV γ rays with the Ge(Li) detector. With the aid of the decay scheme

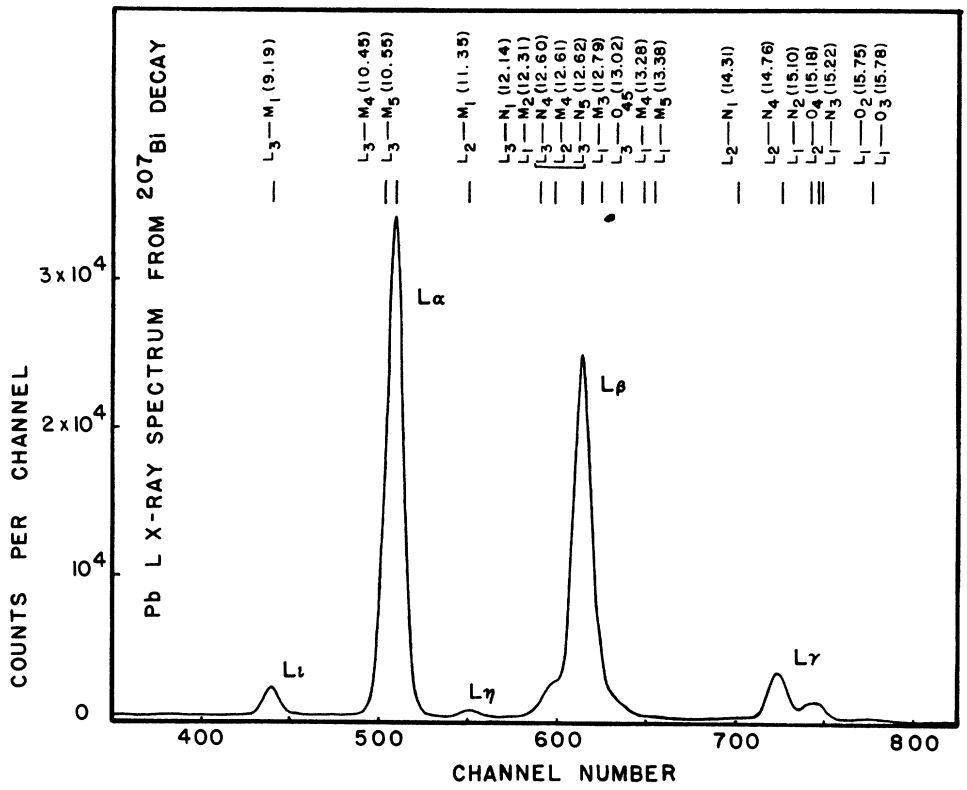

FIG. 2. Singles Pb L-x-ray spectrum from the decay of ^{207}Bi taken with a KeVex Si(Li) x-ray spectrometer having a resolution of 155 eV FWHM at 5.9 keV. Prominent transitions filling the L-shell vacancies and the corresponding energies in keV are included.

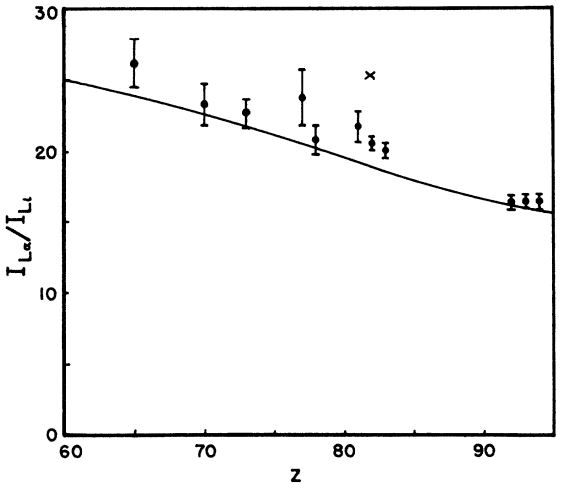

FIG. 3. Ratio of the intensities of $L\alpha$ and Ll x rays ($I_{L\alpha}/I_{Ll}$) vs Z. Solid line represents Scofield's theory. Point × is from Ref. 21.

information available from Ref. 10, we obtain a value of $I_L = 0.364 \pm 0.036$.

III. RESULTS AND DISCUSSION

A. L_2 and L_3 Subshells

The ratio $I_{L\alpha}/I_{Ll}$ of the intensities of $L\alpha$ to Ll x rays was measured for Z values ranging from 65 to 94 and is presented in Table I and Fig. 3. The branching ratios s_2 obtained from the measurement of L-x-ray–$K\alpha_2$-x-ray coincidences are presented in Table II. Figure 4 illustrates the comparison between Scofield's theory[1] and experiment by plotting $s_2(\text{exp})/s_2(\text{theor})$ vs Z. The branching ratios s_3 obtained from the coincidences between L x rays and $K\alpha_1$ x rays are presented in a similar fashion in Table III and Fig. 5.

TABLE I. Ratio (I_α/I_{Ll}) of the intensities of $L\alpha$-to-Ll x rays originating from the filling of L_3-subshell vacancies.

Z	Experiment	Theory: Scofield (Ref. 1)	Theory: Rosner and Bhalla (Ref. 2)
60		25.0	
63			24.4
65	26.2 ± 1.8	23.9	
70	23.3 ± 1.5	22.7	22.5
73	22.7 ± 1.0	21.8	
74		21.3	
77	23.8 ± 2.0		
78	20.8 ± 1.0	20.2	
79		19.9	
80		19.6	19.5
81	21.7 ± 1.1	19.2	
82	20.5 ± 0.5	18.8	
83	20.0 ± 0.5		
90		16.6	
92	16.3 ± 0.5	16.1	
93	16.4 ± 0.5		16.0
94	16.3 ± 0.5		

TABLE II. Comparison of experimental and theoretical values for the radiative branching ratio s_2 for the L_2 subshell.

Z	Radioactive source of x rays	Experiment	Ref.	Theory	Expt / Theory
65	^{159}Dy	0.204 ± 0.024	16	0.177	1.15 ± 0.12
67	^{165}Dy	0.226 ± 0.055	15	0.178	1.24 ± 0.30
68	^{166}Ho	0.202 ± 0.090	15	0.179	1.10 ± 0.50
70	^{170,171}Tm	0.192 ± 0.010	13	0.181	1.06 ± 0.05
73	^{181}W	0.196 ± 0.010	14	0.191	1.03 ± 0.05
76	^{186}Re	0.230 ± 0.023	[a]	0.203	1.15 ± 0.12
77	^{191}Os	0.232 ± 0.023	[a]	0.208	1.12 ± 0.11
80	^{204}Tl	0.243 ± 0.012	12	0.222	1.09 ± 0.06
81	^{203}Hg	0.238 ± 0.012	11	0.228	1.04 ± 0.06
82	^{207}Bi	0.248 ± 0.019	10	0.231	1.07 ± 0.08

[a]Present work.

The theoretical values for s_2 and s_3 are taken from the work of Scofield. The estimated error in these theoretical branching ratios is at most 1.5% at $Z = 80$. Calculations by Lasker and Raffray[21] were available for $Z = 82$ and are included for comparison. Rosner and Bhalla[2] calculated relative intensities but did not include all prominent transitions from higher shells. Hence only $I_{L\alpha}/I_{Ll}$ values were available from their work. It should be noted that the theoretical values for $I_{L\alpha}/I_{Ll}$ by Scofield[1] and Rosner and Bhalla[2] agree with each other, while those of Lasker and Raffray[21] deviate considerably.

The agreement between the present experimental work and theory is reasonable, especially in the case of s_3 (see Fig. 5). However, it is obvious that the majority of the experimental branching ratios tend to lie above the theoretical values by a few percent (see Figs. 3 and 4). It is reasonable to conclude that the theoretical estimates of transition rates involving N, O, ...-shell electrons relative to those of M-shell electrons are consistently smaller than what the experiments indicate. The theoretical transition rate is essentially a measure of

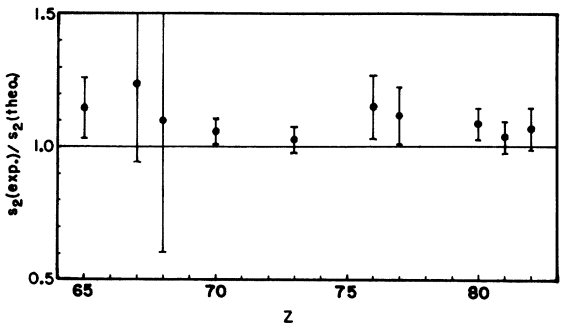

FIG. 4. Ratio of experimental value of s_2 to the theoretical value from Scofield's work is plotted against Z.

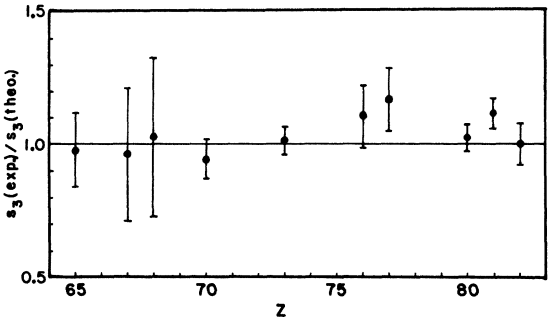

FIG. 5. Ratio of experimental value of s_3 to the theoretical value from Scofield's work is plotted against Z.

the overlap of the initial and final bound-state radial wave functions, and hence we may say that the overlap of the wave function is underestimated in theory in the case of electrons in outer shells compared to that of an electron in an inner shell. One might suspect that the effect of screening has not been properly taken into account. Similarly, this trend in the experimental branching ratios is observed in the work on the K shell, where the ratio $I_{K\beta}/I_{K\alpha}$ of intensities of $K\beta$ x rays involving M, N, O, ...-shell electrons and $K\alpha$ x rays involving L-shell electrons is found to be higher than theoretical predictions. The present results are in qualitative agreement with the work of Goldberg, [22] who measured relative intensities of individual L-x-ray lines with a diffraction spectrometer in the range $73 \leq Z \leq 92$. The ratios for the most prominent transitions filling L_2 and L_3 vacancies are calculated from Goldberg's results and are compared with the ratios calculated from the theoretical estimates by Scofield[1] in Fig. 6. It should be pointed out that the disagreement between theory and experiment is not noticed in the case of $I_{L\gamma 6}/I_{L\gamma 1}$ even though the electrons involved are from two different shells, O and N, respectively.

The situation concerning the relative intensities of transitions which involve electrons from the same outer shell is not very clear. The present results on $I_{L\alpha}/I_{L l}$ involving only electrons from the M shell show a trend similar to that observed above in the case of s_2 and s_3. Goldberg's results clearly show that the agreement between Scofield's work and experiment is reasonable when the vacancy-filling electrons arise from the same shell. The agreement is particularly good when the electrons are from neighboring subshells, as in the case of $I_{L\alpha 1}/I_{L\alpha 2}$ involving M_5 and M_4 electrons. But slight deviations from theory in the case of $I_{K\beta 3}/I_{K\beta 1}$ involving M_3 and M_2 subshell electrons were reported by Salem *et al.*[5] who attributed them to the electron screening effect. A careful and extensive study of the relative intensities is obviously necessary.

TABLE III. Comparison of experimental and theoretical values for the radiative decay branching ratio s_3 for the L_3 subshell.

Z	Radioactive source of x rays	Experiment	Ref.	Theory (Ref. 1)	Expt / Theory
65	^{159}Dy	0.170 ± 0.024	16	0.1728	0.98 ± 0.14
67	^{165}Dy	0.170 ± 0.043	15	0.1735	0.96 ± 0.25
68	^{166}Ho	0.186 ± 0.068	15	0.174	1.03 ± 0.30
70	^{170,171}Tm	0.165 ± 0.009	13	0.175	0.94 ± 0.07
73	^{181}W	0.185 ± 0.010	14	0.183	1.01 ± 0.05
76	^{186}Re	0.217 ± 0.020	[a]	0.195	1.11 ± 0.11
77	^{191}Os	0.233 ± 0.023	[a]	0.200	1.17 ± 0.12
80	^{204}Tl, ^{198}Au	0.217 ± 0.011	12	0.212	1.02 ± 0.05
81	^{203}Hg	0.239 ± 0.012	11	0.216	1.11 ± 0.05
82	^{207}Bi	0.223 ± 0.017	10	0.221	1.00 ± 0.08

[a]Present work.

B. L_1 Subshell

Direct determination of the branching ratio s_1 is not feasible by methods similar to those applied in the case of s_2 and s_3, for the following two reasons: (i) It is not possible to isolate L_1 vacancies by coincidence techniques unless one can use L_1 conversion electrons to signal the L_1 vacancies. Even when such isolation is accomplished, the Coster-Kronig transitions transfer the majority of the va-

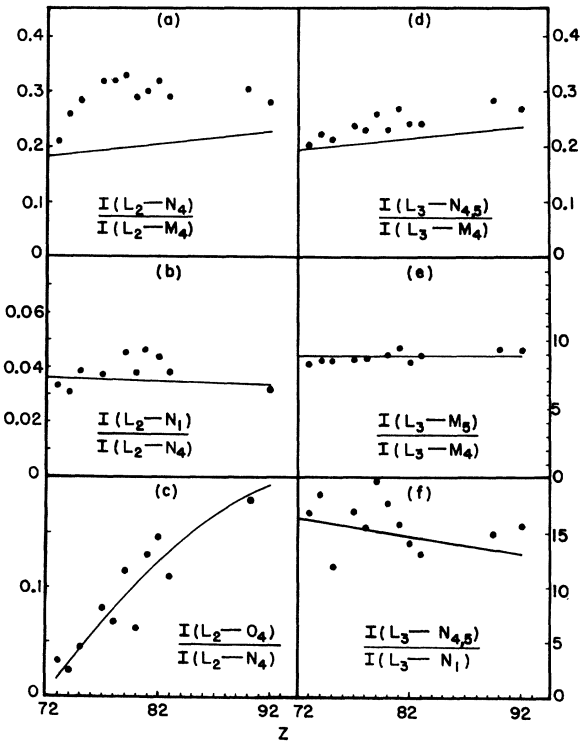

FIG. 6. Ratios of individual transition rates for L_2 and L_3 subshells calculated from Goldberg's experimental work. Solid lines represent the theoretical ratios from Scofield's work.

cancies to the L_2 and L_3 subshells. (ii) The alternative is to study the L-x-ray spectra at very high resolution where L_1 characteristic x rays can be well separated. But the semiconductor detector does not possess high enough resolution.

Since the branching ratio s_1 enters into the determination of L_1-subshell yields (see Refs. 10 and 11), an evaluation of the theoretical values calculated from Scofield's work is very desirable. An indirect procedure is described in the present work to obtain s_1 by analyzing the singles Pb L-x-ray spectrum from the decay of ^{207}Bi (see Fig. 2). The high-energy end of this spectrum is completely characteristic of the L_1 subshell because it contains transitions ($L_1 \rightarrow N$, O) of highest energy. The $L\gamma$ group contains two parts: (i) the L x rays arising from the filling of an L_2 vacancy by N, O, ...-shell electrons, i.e., $L^2\gamma$, and (ii) the L x rays arising from the $L_1 \rightarrow N$, O, ... transitions, i.e., $L^1\gamma$. Figure 7 illustrates the analysis of the $L\gamma$ spectrum into its components $L^2\gamma$ and $L^1\gamma$. The energies of the prominent transitions comprising the $L^2\gamma$ and $L^1\gamma$ peaks were taken from Bearden's tables.[8] Allowance has been made for the small change in the FWHM of the photopeaks with energy. A Hewlett Packard 9100A calculator was used to construct the theoretical shapes assuming Gaussian shapes for the photopeaks. The relative intensities of the transitions within each of the two groups $L^2\gamma$ and $L^1\gamma$ were taken from Scofield. The relative intensities of the two groups were adjusted to give the best fit to the experimental data. And the agreement was

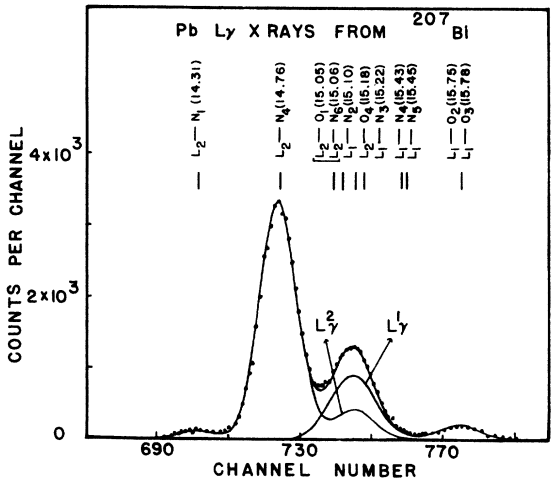

FIG. 7. Analysis of the Pb $L\gamma$ spectrum from the decay of ^{207}Bi into its components $L^1\gamma$ and $L^2\gamma$ from L_1 and L_2 subshells, respectively. Solid curves represent the shapes of the photopeaks calculated from Scofield's theory. Prominent transitions constituting the $L\gamma$ peak and the corresponding energies in keV are included.

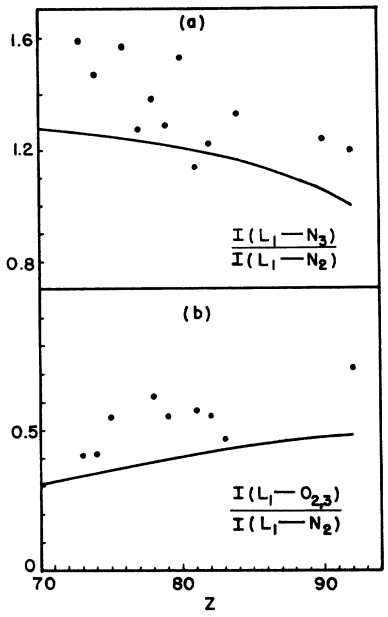

FIG. 8. Ratios of prominent individual transition rates for the L_1 subshell calculated from Goldberg's experimental work. Solid lines represent the theoretical ratios from Scofield's work.

reasonable. Since it is evident from Goldberg's work that the relative intensities of the main transitions comprising the $L^2\gamma$ group agree with Scofield's theory [see Figs. 6(b) and 6(c)], the small deviations observed could only be attributed to the $L^1\gamma$ group, except at the low-energy end where a slight excess of $L\gamma_5$ x rays from the L_2 subshell can be noticed.

We have plotted, in Fig. 8, the ratios of the intensities of prominent transitions comprising the $L^1\gamma$ group from the experimental work of Goldberg and compared them with Scofield's theory. Deviations are indeed substantial, unlike the ratios in the case of the L_2 and L_3 subshells, and thus support the above conclusion that agreement between theory and experiment in the case of $L^1\gamma$ is approximate.

The analysis of the $L\gamma$ peak together with the measurement of the relative intensities of the Ll, $L\alpha$, $L\eta$, $L\beta$, and $L\gamma$ groups yields s_1 from the following relation:

$$s_1 = \frac{C_{L^1\gamma}}{C_{L\eta,\beta} - s_3 C_{Ll,\alpha} - C_{L^2\gamma}(1+s_2)/s_2}, \qquad (4)$$

where $C_{L^1\gamma}$ is the number of counts in the $L^1\gamma$ peak, $C_{L^2\gamma}$ is the number of counts in the $L^2\gamma$ peak, $C_{L\eta,\beta}$ is the total number of counts in the $L\eta$ and $L\beta$ peaks, and $C_{Ll,\alpha}$ is the total number of counts in Ll and $L\alpha$ peaks. All the counting rates C are corrected for the photopeak efficiency and attenuation effects.

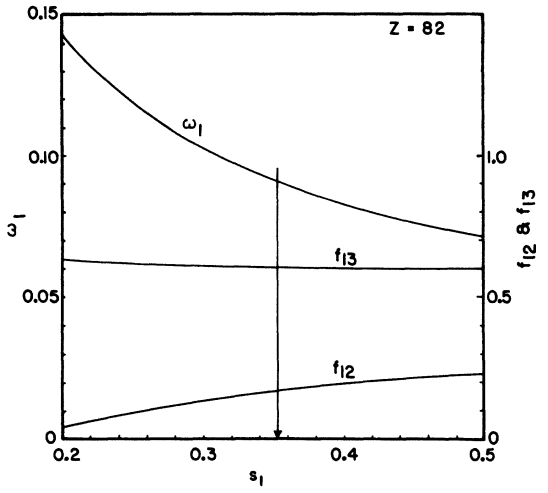

FIG. 9. Dependence of L_1-subshell yields on the radiative decay branching ratio s_1. Arrow indicates the present work.

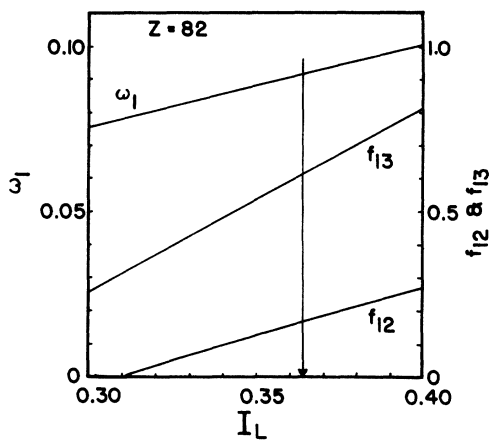

FIG. 10. Dependence of L_1-subshell yields on I_L, the number of L x rays per decay of ^{207}Bi. Arrow indicates the present work.

Experimental values for s_2 and s_3 are previously available (Tables II and III). The value obtained for s_1 at $Z = 82$ from the present work is 0.353 ± 0.053. The theoretical estimate by Scofield is 0.315.

With the knowledge of s_1 we proceed now to determine the L_1-subshell yields. If the number of L_i-subshell vacancies created per decay is given by a_i, and I_L is the total number of L x rays emitted from all the subshells per decay and $C_L = C_{Ll} + C_{L\alpha} + C_{L\eta} + C_{L\beta} + C_{L\gamma}$, the following relations can be established to obtain L_i-subshell yields:

$$\omega_1 = \frac{1}{a_1}\left[C_{L1_\gamma}\left(\frac{1+s_1}{s_1}\right)\frac{I_L}{C_L}\right], \tag{5}$$

$$\omega_1 + f_{12}\omega_2 = \frac{1}{a_1}\left([C_L - C_{Ll,\alpha}(1+s_3)]\frac{I_L}{C_L} - a_2\omega_2\right), \tag{6}$$

$$f_{13} + f_{12}f_{23} = \frac{1}{a_1}\left(C_{Ll,\alpha}\frac{(1+s_3)}{\omega_3}\frac{I_L}{C_L} - a_2 f_{23} - a_3\right). \tag{7}$$

The a_i are calculated from the knowledge of the decay scheme of ^{207}Bi and the procedure for the calculation was explained in Ref. 10. Experimental values of s_2, s_3, ω_2, and ω_3 are also available from Ref. 10. A summary of the quantities obtained from the literature and the values of L_1 yields obtained in the present work are given in Table IV. The agreement between L_1 yields of the present work and the previous values obtained from coincidence measurements is reasonable. The interrelationship between the two experimental quantities s_1 and I_L and the L_1-subshell yields is presented in Figs. 9 and 10. It is obvious that changes in the three L_1 yields accompany variations in s_1 or I_L in a distinctly different manner, while only f_{13} is independent of large errors in s_1.

TABLE IV. Summary of the measured quantities on Pb L-shell yields from ^{207}Bi decay.

	Present work	Ref. 10
	$s_1 = 0.353 \pm 0.053$	$s_2 = 0.248 \pm 0.019$
	$I_L = 0.364 \pm 0.036$	$s_3 = 0.223 \pm 0.017$
	$C_L{}^1{}_\gamma / C_L = 0.020 \pm 0.004$	$\omega_2 = 0.364 \pm 0.015$
	$C_{Ll,\alpha}/C_L = 0.478 \pm 0.020$	$\omega_3 = 0.315 \pm 0.013$
		$f_{23} = 0.164 \pm 0.016$
ω_1	0.09 ± 0.02	0.07 ± 0.02
f_{12}	0.17 ± 0.05	0.15 ± 0.04
f_{13}	0.61 ± 0.08	0.57 ± 0.03

One serious limitation to the application of this method for the study of L_1-subshell vacancies is the effect of Coster-Kronig transitions that depopulate L_1 vacancies, thus yielding a relatively small number of L_1 x rays. However, in the middle-Z region (50–73) L_1–L_3X transitions are fewer in number because $X = M$ shell electrons cannot participate in the transition and a high-resolution study of singles spectra can yield results on the L_1 subshell in this region.

IV. SUMMARY

Experimental relative intensities of L x rays from individual L subshells are compared with theoretical calculations by Scofield and Rosner and Bhalla. There is reasonable evidence to suggest that transitions involving outer-shell ($N, O, \ldots$) electrons compared to inner-shell (M) electrons are underestimated in the theory.

ACKNOWLEDGMENTS

The authors wish to acknowledge the cooperation of R. S. Frankel and G. W. Kramer of KeVex

Corporation for permitting us to use two of their best resolution Si(Li) x-ray detectors. The kind assistance of M. L. Hyder, J. W. Morris, and M. A. Wakat of Savannah River Laboratory in providing us transuranium isotope sources is acknowledged. The authors also acknowledge the assistance of J. T. West in analyzing some of the data.

*Work supported by USAROD basic research grant No. DA-ARO-D31-124-70-G78.

[1]J. H. Scofield, Phys. Rev. 179, 9 (1969).
[2]H. R. Rosner and C. P. Bhalla, Z. Physik 231, 347 (1970); supplementary tables NAPS Document No. 00739 (National Auxiliary Publications Service, New York, 1969).
[3]P. J. Ebert and V. W. Slivinsky, Phys. Rev. 188, 1 (1969).
[4]G. C. Nelson and B. G. Saunders, Phys. Rev. 188, 108 (1969).
[5]S. I. Salem, B. G. Saunders, and G. C. Nelson, Phys. Rev. A 1, 1563 (1970).
[6]V. W. Slivinsky and P. J. Ebert, Phys. Letters 29A, 463 (1969).
[7]J. S. Hansen, H. U. Freund, and R. W. Fink, Nucl. Phys. A142, 604 (1970).
[8]J. A. Bearden, Rev. Mod. Phys. 39, 1 (1967).
[9]P. Venugopala Rao, in *Proceedings of the International Conference on Electron Capture and Higher Order Processes in Nuclear Decay, Hungary* (Eötvös Lóránd Phys. Soc., Budapest, 1968).
[10]P. Venugopala Rao, R. E. Wood, J. M. Palms, and R. W. Fink, Phys. Rev. 178, 1997 (1969).
[11]R. E. Wood, J. M. Palms, and P. Venugopala Rao, Phys. Rev. 187, 1497 (1969).
[12]J. M. Palms, R. E. Wood, P. V. Rao, and V. O. Kostroun, Phys. Rev. C 2, 592 (1970).
[13]S. Mohan, H. U. Freund, R. W. Fink, and P. Venugopala Rao, Phys. Rev. C 1, 254 (1970).
[14]S. Mohan, R. W. Fink, R. E. Wood, J. M. Palms, and P. Venugopala Rao, Z. Physik 239, 423 (1970).
[15]C. P. Holms and V. O. Kostroun, Bull. Am. Phys. Soc. 15, 561 (1970).
[16]J. C. McGeorge, H. U. Freund, and R. W. Fink, Nucl. Phys. A154, 526 (1970).
[17]P. Venugopala Rao and B. Crasemann, Phys. Rev., 139, 1926 (1965).
[18]J. M. Palms, R. E. Wood, and P. Venugopala Rao, Nucl. Instr. Methods (to be published).
[19]D. A. Landis, F. S. Goulding, and R. H. Pehl, IEEE Trans. Nucl. Sci. (to be published).
[20]J. M. Palms, P. Venugopala Rao, and R. E. Wood, Nucl. Instr. Methods 64, 310 (1968).
[21]W. Lasker and Y. Raffray, Compt. Rend. 265, 1307 (1967).
[22]M. Goldberg, Ann. Phys. (Paris) 7, 329 (1962).

PHYSICAL REVIEW A VOLUME 3, NUMBER 5 MAY 1971

Application of the Projection Technique to Two-Level Atoms

A. Muriel
Department of Physics, Towson State College, Towson, Maryland 21204
(Received 16 September 1970)

Exact, formal, and usable solutions of the Liouville equation corresponding to the problem of independent two-level atoms in an external field are presented. Two examples are worked out: calculation of the polarization, and a model of pumping or population inversion by a δ-function external field. The relation of the solutions to other problems in statistical mechanics is also discussed.

I. INTRODUCTION

In the past few years, exact solutions of the Liouville equation or the von Neumann equation have become available.[1,2] The mathematical structure of these model-dependent solutions is such that the techniques used could be applied to solutions of simpler, but also important, problems. The techniques vary somewhat, but because of the use of 2×2 matrices, a direct technique employing projection operators is particularly direct and straightforward.[3]

The basic physical problem considered is a system of noninteracting two-level atoms. Transitions between the two levels of an atom occur only because of the presence of an external field. This kind of interaction is expressed by a Hamiltonian of the form

$$H=\begin{pmatrix} \omega_1 & -pE \\ -pE & \omega_2 \end{pmatrix}, \tag{1}$$

where $E(t)$ is a time-dependent external field. If E is constant, the problem is trivial.[4]

There are two ways of solving the problem. The Schrödinger equation may be solved,[5] or we may solve the Liouville equation. The two approaches are of course related, but we shall use the latter approach because of some possible applications in the construction of laser models.